HHS Public Access

Author manuscript

Chem Res Toxicol. Author manuscript; available in PMC 2020 February 23.

Published in final edited form as:

Chem Res Toxicol. 2019 March 18; 32(3): 474–483. doi:10.1021/acs.chemrestox.8b00346.

Aromatic Residues at the Dimer–Dimer Interface in the Peroxiredoxin Tsa1 Facilitate Decamer Formation and Biological Function

Matthew A. Loberg[†], **Jennifer E. Hurtig**[†,§], **Aaron H. Graff**[‡], **Kristin M. Allan**[†], **John A. Buchan**[†], **Matthew K. Spencer**[†], **Joseph E. Kelly**[†], **Jill E. Clodfelter**[‡], **Kevin A. Morano**[§], **W. Todd Lowther**[‡], **James D. West**[*,†]

[†] Biochemistry & Molecular Biology Program, Departments of Biology and Chemistry, The College of Wooster, Wooster, Ohio 44691, United States

[‡] Department of Biochemistry and Center for Structural Biology, Wake Forest School of Medicine, Winston-Salem, North Carolina 27101, United States

[§] Department of Microbiology & Molecular Genetics, McGovern Medical School, The University of Texas Health Science Center at Houston, Houston, Texas 77030, United States

Abstract

To prevent the accumulation of reactive oxygen species and limit associated damage to biological macromolecules, cells express a variety of oxidant-detoxifying enzymes, including peroxiredoxins. In *Saccharomyces cerevisiae*, the peroxiredoxin Tsa1 plays a key role in peroxide clearance and maintenance of genome stability. Five homodimers of Tsa1 can assemble into a toroid-shaped decamer, with the active sites in the enzyme being shared between individual dimers in the decamer. Here, we have examined whether two conserved aromatic residues at the decamer–building interface promote Tsa1 oligomerization, enzymatic activity, and biological function. When substituting either or both of these aromatic residues at the decamer–building interface with either alanine or leucine, we found that the Tsa1 decamer is destabilized, favoring dimeric species instead. These proteins exhibit varying abilities to rescue the phenotypes of oxidant sensitivity and genomic instability in yeast lacking Tsa1 and Tsa2, with the individual leucine substitutions at this interface partially complementing the deletion phenotypes. The ability of Tsa1 decamer interface variants to partially rescue peroxidase function in deletion strains is temperature-dependent and correlates with their relative rate of reactivity with hydrogen peroxide and their ability to interact with thioredoxin. Based on the combined results of in vitro and in vivo assays, our findings indicate that multiple steps in the catalytic cycle of Tsa1 may be impaired by introducing

[*]**Corresponding Author:** Tel.: (330) 263-2368. Fax: (330) 263-2378. jwest@wooster.edu.

The authors declare no competing financial interest.

ASSOCIATED CONTENT

Supporting Information

The Supporting Information is available free of charge on the ACS Publications website at DOI: 10.1021/acs.chemrestox.8b00346. Primers used for site-directed mutagenesis (Table S1); effect of Tsa1 variants on suppressing elevated mutation rates in yeast lacking Tsa1 and Tsa2 (Table S2); protein expression levels of Tsa1 variants in mid-log phase and stationary phase cells (Figure S1); alterations in DVSF-mediated cross-linking patterns among Tsa1 decamer interface variants (Figure S2) (PDF)

substitutions at its decamer–building interface, suggesting a multifaceted biological basis for its assembly into decamers.

Graphical Abstract

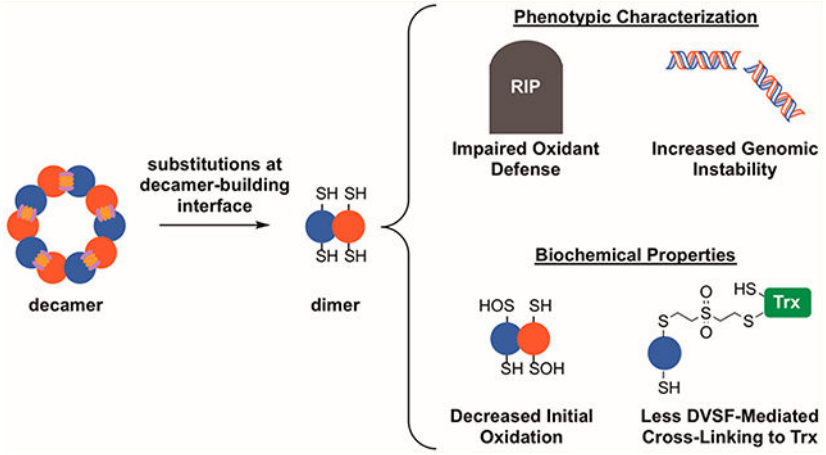

Elevated levels of oxygen-based oxidants, collectively termed reactive oxygen species (ROS), bring about a broad range of biological effects. The production of ROS can be increased in several ways, including aberrant mitochondrial electron transport, signaling by certain growth factors, or stimuli that activate the innate immune response.[1,2] Depending on the source and magnitude of ROS production, their biological effects range from alteration of signal transduction pathways that promote cell growth, differentiation, or stress adaptation to more detrimental effects that include genomic instability and cell death.[3–6] The physiological effects of ROS are closely tied to the oxidation of various biological macromolecules, including specific sites in DNA and proteins.[7–10] To signal the accumulation of low levels of ROS and counteract the toxic effects observed at high ROS concentrations, cells express several oxidant defense enzymes, including a conserved family of cysteine-dependent peroxidases called peroxiredoxins.[11,12]

Peroxiredoxins from different species employ a thiol-based mechanism to detoxify peroxides. All peroxiredoxins use a catalytic (i.e., peroxidatic) cysteine that undergoes oxidation to a cysteine sulfenic acid (Cys-SOH) upon reaction with a peroxide.[13] In most peroxiredoxins, the Cys-SOH intermediate subsequently condenses with a nearby thiol group in a resolving cysteine, commonly found on a different subunit of the enzyme, to form a disulfide bond.[14] Intersubunit disulfides formed upon peroxiredoxin oxidation are most commonly reduced by the thioredoxin system.[15] Despite the commonalities in their chemical mechanism, peroxiredoxins have diverged throughout evolution, with family members exhibiting different quaternary structures, substrate specificities, mechanisms of catalysis, three different biochemical activities (i.e., peroxidase activity, redox signaling activity, and molecular chaperone activity), and subcellular localizations.[16–19] For instance, some peroxiredoxins form constitutive homodimers, whereas others form toroid-shaped decamers that assemble from a pentamer of catalytic dimers.[16,20]

Baker's yeast, *Saccharomyces cerevisiae*, provides a useful model system for studying the structural, biochemical, and functional characteristics of peroxiredoxins. Of the five peroxiredoxins in *S. cerevisiae*, three family members—Ahp1, Tsa1, and Tsa2—reside in the cytosol, where they protect against oxidant-mediated toxicity.[21–23] Of these, Tsa1 and Ahp1 are expressed at the highest levels,[24] but they exhibit distinct substrate preferences, with Ahp1 preferentially detoxifying organic peroxides and Tsa1 having a broader substrate utilization.[22,25] Ahp1 and Tsa1 also differ in the oligomeric states that they form. Ahp1, which is an atypical 2-Cys peroxiredoxin, forms a stable, constitutive dimer that utilizes an A-type interface (Figure 1A).[26] In contrast, Tsa1 (a typical 2-Cys peroxiredoxin) exists as a dimer that utilizes a B-type interface.[27] Tsa1 dimers can further oligomerize to form decamers using a separate A-type interface. Importantly, the oligomeric state of Tsa1 is influenced by the many oxidation states of its active cysteine residues (e.g., disulfide-linked dimers, reduced decamers, or multimerized decamers (i.e., high-molecular-weight complexes) that form upon hyperoxidation).[27–29] Similar redox-dependent structural states have been observed for typical 2-Cys peroxiredoxins from a variety of species.[20,30]

Previously, we identified a pair of highly conserved aromatic residues at the A-type interface in Ahp1 that promotes dimer stabilization, biological function, and intersubunit cross-linking by a thiol-reactive cross-linker.[31] We proposed that these residues are involved in hydrophobic interactions and/or π-stacking interactions as a means of contributing to dimer formation. This aromatic interface is found at the decamer–building (or dimer–dimer) interface among the decameric peroxiredoxins, as deduced both from primary sequence alignments and structural comparisons (Figures 1A and 1B). Here, we conducted a mutagenesis-based study to probe the structural and functional significance of these aromatic residues in Tsa1. We report that substitution of either of these aromatic residues at the decamer–building interface (i.e., F44 or Y78) with smaller aliphatic residues (e.g., Ala, Leu) disrupts the decamer formed by Tsa1 in its reduced state and compromises its ability to protect cells against oxidant-mediated toxicity and genomic instability, perhaps through the combined effects of slow reactivity with peroxides and decreased interaction with thioredoxins.

MATERIALS AND METHODS

Molecular Biology

Constructs for expression of wt Tsa1 in yeast (p416-GPD) and bacteria (pET45b) have been reported previously.[32] For yeast experiments, genes encoding wild-type Tsa1 or Tsa1 decamer interface variants (all with an *N*-terminal FLAG tag) were placed under the control of the GPD promoter, which allows for constitutive, high-level expression in yeast.[31,32] For bacterial over-expression, the Tsa1 gene was tagged at the N-terminus with a vector-encoded 6X-His tag. Codons for aromatic residues at the decamer interface in Tsa1 were mutated to Ala or Leu using the QuikChange mutagenesis protocol (Agilent) with the primers reported in Table S1 in the Supporting Information, as described previously.[31,32] All constructs containing mutations were verified by DNA sequencing.

Expression and Purification of Tsa1 Interface Variants

pET45b constructs containing wild-type (wt) and mutant Tsa1 genes were transformed in C41(DE3) *Escherichia coli* cells. Media (4 L of LB broth containing 100 μg/mL ampicillin) were inoculated with bacterial strains, grown to mid log phase, and induced for 18 h at 37 °C with 300 μM IPTG. Protein lysates were prepared by resuspending cell pellets in 100 mL lysis buffer (50 mM HEPES (pH 7.9), 500 mM KCl, 5 mM imidazole, 10% (v/v) glycerol, 0.1% (v/v) Triton X-100, 1 mM $MgCl_2$, 100 μM DNase I, 100 μM phenylmethylsulfonyl fluoride, and 100 μM benzamidine) and passing this mixture through an Emulsiflex-C3 homogenizer (Avestin). Lysates were cleared of debris by centrifuging samples twice at 39 000g for 30 min at 4 °C. Cleared supernatants were loaded onto a column packed with HisPur Cobalt Superflow Agarose (Thermo-Scientific) and subjected to gradient elution in 50 mM HEPES (pH 7.9), 500 mM KCl, and 5–250 mM imidazole. Fractions containing Tsa1 were pooled, dialyzed against 4 L of gel filtration buffer (20 mM HEPES (pH 7.5) and 100 mM NaCl), and concentrated. Proteins were further purified on a Superdex 200 gel filtration column. Fractions containing pure Tsa1 were pooled, concentrated, and exchanged into protein storage buffer (50 mM Tris-HCl (pH 7.5), 2 mM DTT, 10% glycerol, 100 μM phenylmethylsulfonyl fluoride, and 100 μM benzamidine) prior to storage at −80 °C. Proteins were quantified at 280 nm using an estimated extinction coefficient of 23 950 M^{-1} cm^{-1} (https://web.expasy.org/protparam/).

Analysis of Recombinant Tsa1 Oligomeric States

Approximate molecular weights of Tsa1 complexes were determined by native PAGE as previously described[31] and by using size exclusion chromatography coupled with multiangle light scattering (SECMALS) analysis. For SEC-MALS experiments, proteins were diluted to 100 μM in SEC-MALS buffer (50 mM HEPES, pH 7.5, 100 mM NaCl, and 1 mM tris(2-carboxyethyl)phosphine hydrochloride prior to resolution on a TSK Gel 4000 SW gel filtration column (8 μm particle size, 7.8 × 30 cm, Tosoh Biosciences). Chromatographic separation was performed over 35 min at a flow rate of 0.5 mL/min, monitoring elution spectrophotometrically at A_{280} and MALS using a HELIOS II detector (Wyatt Technology). Molecular weights were estimated for prominent peaks (determined from the A_{280} traces) from MALS data using Astra 6 software (Wyatt Technology).

Immunoblotting and Immunoprecipitation Analysis of Tsa1 Variants Expressed in Yeast Cells

Procedures for lysing yeast cells and immunoblotting have been reported previously.[33] Briefly, yeast cells expressing wt Tsa1 or decamer interface variants were grown to mid log phase and lysed with acid-washed glass beads under nondenaturing conditions in lysis buffer (20 mM Tris (pH 8.0), 0.5 mM EDTA, 10% glycerol, 50 mM NaCl, and Protease Arrest protease inhibitor cocktail (G-Biosciences)). Immunoblots were conducted using reducing SDS-PAGE prior to transfer onto PVDF and detection with antibodies against the FLAG epitope (Sigma), TAP tag (antiprotein A, Sigma), or Pgk1 (Invitrogen). Where indicated, quantification of protein expression was performed on digital images of immunoblots using Fiji software, normalizing to Pgk1 expression as a loading control.[34] For immunoprecipitation of Tsa1 with cross-linked binding partners, cells were grown to mid

log phase and treated for 1 h at 30 °C with the cross-linker divinyl sulfone (DVSF, 1 mM). Subsequently, immunoprecipitation of Tsa1 from yeast lysates was performed with anti-FLAG beads as previously described.[31,32] Immunoprecipitates were probed for cross-links between TAP-tagged Trx2 and FLAG-tagged Tsa1 variants using immunoblot.

Protection of Tsa1 Interface Variants against Peroxide-Mediated Toxicity

Wild-type (BY4741) and *tsa1*- and *tsa2*-deficient (*tsa1*Δ*tsa2*Δ) yeast were transformed with p416-GPD or p416-GPD containing genes encoding FLAG-tagged Tsa1. The ability of Tsa1 variants to protect against H_2O_2 was monitored as previously described.[31,32] Briefly, stationary phase cultures were diluted serially in 150 mM NaCl from OD_{600} of 0.5. Dilutions were spotted on plates containing YPD growth medium or YPD containing 4 mM H_2O_2. Plates were incubated at 30 or 37 °C for 48 h.

Protection of Tsa1 Interface Variants against Genomic Instability

To determine the effect of decamer interface substitutions on genomic stability in yeast, *tsa1*Δ*tsa2*Δ strains expressing the tagged variants of Tsa1 were monitored for fluctuation in the *CAN1* gene, as described elsewhere.[35] Briefly, yeast cultures were grown in SC-Ura medium overnight at 30 °C to saturation. The following day, cultures were diluted by a factor of 10^6 in SC-Ura and grown for an additional 48 h at 30 °C. Subsequently, cultures (100 μL) were plated on SC-Ura-Arg plates containing 60 μg/mL canavanine sulfate and grown for 72 h at 30 °C. To measure viability on the same cultures, cultures were diluted by a factor of 10^5 from which 100 μL were plated on SC-Ura plates and grown for 48 h at 30 °C. Colonies on both fluctuation analysis plates and viability plates were counted. Mutation rates and corresponding 95% confidence intervals were determined by the method of the median.

Determining the Second-Order Rate Constant for Reaction with of Tsa1 Decamer Interface Variants with H_2O_2

Competitive peroxide binding assays were performed between Tsa1 and horseradish peroxidase (HRP) using a modified published procedure.[36] Briefly, Tsa1 variants were reduced with 20 mM DTT for 30 min at room temperature, exchanged into buffer containing 5 mM K_3PO_4 (pH 7.0) and 0.1 mM diethylenetriaminepentaacetic acid using Biospin 6 columns (BioRad), and quantified at A_{280}. HRP (Sigma) was dissolved in buffer containing 5 mM K_3PO_4 (pH 7.0) and 0.1 mM diethylenetriaminepentaacetic acid and quantified at 403 nm (extinction coefficient = 102 000 M^{-1} cm^{-1}). Reactions mixtures (150 μL) containing 5 mM K_3PO_4 (pH 7.0), 0.1 mM DTPA, 7.5 μM HRP, and 0–100 μM reduced Tsa1 were set up in individual wells of a 96-well plate. Reactions were initiated by adding 15 μL of 45 μM H_2O_2, followed by monitoring the decrease in absorbance in each well at 403 nm within 15 s of H_2O_2 addition. Reactions were conducted in quadruplicate. Second-order rate constants for Tsa1 reaction with H_2O_2 were calculated for each reaction using the following equation:

$$\left(\frac{F}{1-F}\right)k_{\mathrm{HRP}}[\mathrm{HRP}] = k_{\mathrm{Tsal}}[\mathrm{Tsa1}]$$

Where $F/(1 - F)$ is the ratio of oxidized HRP (as measured by ΔA_{403}) and $k_{HRP} = 1.7 \times 10^7$ M^{-1} s^{-1}. Results were plotted as a linear expression, with the rate constant for H_2O_2 reactivity (k_{SOH}) being the slope.

Nonreducing Gel Analysis of Tsa1 Oxidation

Disulfide bond formation in Tsa1 variants was monitored via nonreducing electrophoresis as modified from a previously published procedure.[32] Briefly, Tsa1 variants were reduced, exchanged into 5 mM K_3PO_4 (pH 7.0) and 0.1 mM diethylenetriaminepentaacetic acid, and quantified as described above. Reactions (20 μL) containing 10 μM protein, 5 mM K_3PO_4 (pH 7.0), 0.1 mM diethylenetriaminepentaacetic acid, and either buffer or 15 μM H_2O_2 were conducted at room temperature for varying times (0–120 s). Reactions were terminated by the addition of 10 μL of 3X nonreducing Laemmli sample buffer supplemented with 150 mM N-ethylmaleimide, prior to incubation at 95 °C for 5 min. Samples were resolved using SDS-PAGE and visualized with Coomassie Brilliant Blue.

RESULTS

Conserved Aromatic Residues Promote Tsa1 Oligomerization

We previously reported that combined mutation of two conserved aromatic residues (Phe58 and Phe95) at the dimer interface of Ahp1 partially disrupted its ability to form dimers.[31] Upon analysis of the crystal structures of decameric peroxiredoxins such as Tsa1, we noted a similar conserved interface that may contribute to decamer formation (Figure 1). To assess the role that conserved aromatic residues residing at this interface (i.e., Phe44 and Tyr78) play in Tsa1 oligomerization and protein function, these residues were substituted with Ala or Leu (a branched aliphatic side chain capable of stronger hydrophobic interactions) either individually ($F^{44}A$, $Y^{78}A$, $F^{44}L$, or $Y^{78}L$) or in tandem (FYA {or $F^{44}A,Y^{78}A$}, FYL {or $F^{44}L,Y^{78}L$}). Purified proteins with substitutions at this interface electrophoresed principally as dimers by native PAGE, whereas wt Tsa1 migrated at a molecular weight consistent with decameric structure (Figure 2A). The purified proteins were analyzed with SEC-MALS to further confirm their oligomeric states. Wild-type (wt) Tsa1 eluted principally as a decamer (based on its retention time of 19 min and its predicted molecular weight of 227 kDa); however, most Tsa1 variants with substitutions at the interface eluted over a broader time range, with a prominent dimer peak (of ~40–45 kDa) eluting at 24 min (Figure 2B, Table 1). A peak eluting at the same retention time as the decamer was observed for the individual Leu substitutions, although the estimated molecular weights suggested these species were weakly associated or partially assembled decamers. While the slight discrepancies between the native PAGE and SEC-MALS experiments may be due to differences in protein concentrations used in each assay, these results, taken together, indicate that mutation of the conserved aromatic residues at the decamer–building interface disrupt or weaken the decameric state of Tsa1 under reducing conditions.

Substitution of Aromatic Residues at the Decamer–Building Interface in Tsa1 Compromises the Protein's Biological Activity

Yeast lacking Tsa1 and Tsa2 (*tsa1*Δ*tsa2*Δ) exhibit numerous phenotypes, including peroxide sensitivity and genomic instability.[23,35,37] To determine whether substitutions at the decamer

interface influence biological activity, we ectopically expressed these Tsa1 variants in *tsa1*Δ*tsa2*Δ yeast, finding that, overall, variant proteins expressed at slightly decreased, but largely similar, levels when compared with wt Tsa1 in both mid log phase cells and stationary phase cells (see Figure 3A, as well as Figure S1 in the Supporting Information). Each decamer/interface variant of Tsa1 exhibited a decreased ability to defend against oxidative stress (Figure 3B), with proteins harboring $Y^{78}A$ or individual Leu substitutions having an intermediate phenotype. Moreover, these variant proteins failed to suppress mutation rates to the extent that wt Tsa1 did (see Figure 3C and Table S2 in the Supporting Information). As noted with the peroxide sensitivity phenotype, the $Y^{78}A$, $F^{44}L$, and $Y^{78}L$ variants of Tsa1 were capable of partially complementing the mutator phenotype associated with the loss of Tsa1 and Tsa2.

Because the individual Leu substitutions at the decamer interface showed a partial complementation of the peroxide sensitivity phenotype in *tsa1*Δ*tsa2*Δ strains, we tested whether the Leu variants were functional at higher temperatures, as partially assembled Tsa1 decamers may, in theory, be destabilized with increasing heat. The $F^{44}L$ and $Y^{78}L$ variants did not compensate for the lack of Tsa1 and Tsa2 at 37 °C (Figure 4A), suggesting that the weakened decamers formed by these proteins can be inactivated in a temperature-sensitive manner. Moreover, the steady-state levels of these proteins are only slightly changed when switching from lower to higher growth temperatures (Figure 4B), indicating that the monomeric or dimeric Tsa1 complexes are not destabilized or rapidly degraded at higher temperatures.

Substitution of Aromatic Residues at the Decamer–Building Interface in Tsa1 Result in Slow Oxidative Half Reaction

As noted earlier, Tsa1 undergoes a multistep catalytic cycle that involves binding to a peroxide substrate, oxidation of the catalytic cysteine (Cys48) to a cysteine sulfenic acid, condensation with the resolving cysteine (Cys171) to form an intersubunit disulfide, recognition and binding by thioredoxin, and a multistep reduction of the intersubunit disulfide by thioredoxin. If one or several of these steps is/are impaired upon disruption of the decamer, cells would be less able to protect against oxidants. To ascertain which parts of the catalytic cycle might be affected by introducing substitutions at the decamer–building interface, we performed assays aimed at probing the oxidative and reductive steps within the catalytic cycle. A competitive kinetic assay to monitor initial oxidation by H_2O_2 was used with HRP, whereby we estimated the approximate second-order rate constant of reactivity between H_2O_2 and Tsa1 (k_{SOH}). In this assay, wt Tsa1 yielded a rate constant (1.5×10^7 M^{-1} s^{-1}, Figure 5A and Table 2) similar to that reported in the literature (2.2×10^7 M^{-1} s^{-1}).[36] Each of the decamer interface variants tested had a second-order rate constant of reactivity with H_2O_2 between 10-fold and 100-fold lower than that of the wt protein (Figure 5A, Table 2), although these values may be overestimated as noted previously.[38] The most impaired reactivity was observed in the $F^{44}A$, FYA, and FYL variants; however, the $Y^{78}A$, $F^{44}L$, and $Y^{78}L$ proteins exhibited an intermediate level of reactivity with H_2O_2. These trends of peroxide reactivity closely mirrored the ability of each protein to protect against peroxide-mediated toxicity and mutations *in vivo*.

To examine the oxidative half-reaction in another way, we monitored the timing of intersubunit disulfide formation with Tsa1 upon oxidation by peroxide. After prereduction with DTT, all proteins were incubated with peroxide from 15 s to 120 s. The wt protein was oxidized almost completely to form the disulfide within the first 15 s (Figure 5B, as visualized by nonreducing SDS-PAGE); however, disulfide formation in the decamer interface mutants occurred more slowly and failed to go to completion over the time tested, consistent with the slower k_{SOH} rate. These results indicate that Tsa1 mutants lacking aromatic residues at the decamer interface have an impaired ability to perform one or more steps in the oxidative half-reaction of the catalytic cycle.

Decamer Interface Mutants Exhibit Decreased Cross-Linking with Thioredoxins in Vivo

To determine if the mutants of Tsa1 exhibit defects in the reductive phase of reaction, yeast expressing these variants were treated with the bifunctional electrophile divinyl sulfone (DVSF). We have previously shown that Tsa1 undergoes both intersubunit cross-linking and cross-linking to cytosolic thioredoxins (e.g., Trx1 and Trx2) in yeast treated with DVSF (Figure 6A), as a means of irreversibly trapping natural redox partners in complex with each other.[31,32] In particular, our mass spectrometry-based identification experiments indicated that the cross-linked complex at ~35 kDa consisted of Tsa1 linked to Trx2, the two bands at ~46 kDa represent the cross-linked dimer, and the band at ~58 kDa contains a cross-linked Tsa1 dimer linked to Trx2.[32] Therefore, this cross-linking approach was used to monitor in vivo interactions between Trx2 and decamer interface variants of Tsa1. Initially, we found that all decamer interface variants of Tsa1 form lower amounts of a ~35 kDa complex (i.e., Trx2-Tsa1 complex) in DVSF-treated cells (Figure S2 in the Supporting Information). To study the composition of these complexes more fully, two constitutively dimeric forms of Tsa1 (e.g., FYA and FYL) were introduced into yeast lacking the cytosolic thioredoxins (*trx1*Δ*trx2*Δ, or *trx*Δ), and the DVSF cross-linking profiles were compared to those observed in wild-type (BY4741) cells. The results obtained suggested, as noted in our earlier experiments, that FYA and FYL forms of Tsa1 undergo limited cross-linking to Trx1 and Trx2, as the band at ~35 kDa was principally observed in BY4741 cells expressing wt Tsa1 but not FYA and FYL variants (Figure 6B). Instead of undergoing cross-linking with Trx1 and Trx2, FYA and FYL variants of Tsa1 appear to undergo almost quantitative intersubunit cross-linking.

We also monitored cross-linking between Trx2 and Tsa1 variants using coimmunoprecipitation by expressing FLAG-tagged Tsa1 variants in yeast cells expressing a TAP-tagged Trx2. Upon immunoprecipitation of Tsa1 variants from DVSF-treated cells, we found that the wt form of Tsa1 undergoes cross-linking to Trx2 to form at least three higher-molecular-weight complexes (Figure 6C); however, complexes migrating at the same molecular weights were less abundant in immunoprecipitates of the FYA and FYL forms of Tsa1 (Figure 6C). Collectively, these results suggest that Tsa1 variants with substitutions of aromatic residues at the decamer interface interact less favorably with Trx2, indicating that the reductive half-reaction of the peroxiredoxin cycle may be impaired when substitutions are introduced at this interface.

DISCUSSION

In the present study, we describe a mutational analysis of two conserved aromatic residues at the decamer–building interface in Tsa1. Individual or combined substitution of these residues with smaller, hydrophobic residues favors the dimeric oligomeric state and results in decreased biochemical and cellular activity. Earlier comparison of peroxiredoxin structures has revealed that the selected aromatic residues at this interface may be of structural and functional significance. These sites are highly conserved in both typical and atypical 2-Cys peroxiredoxins, both from a primary sequence and structural perspective.[30] Despite their conservation, peroxiredoxins evolved to orient their active sites around this A-type interface differently, with members of the typical class using it to form a toroid-shaped decamer and members of the atypical class using it as an ancestral dimerization interface.[39] In contrast, certain members of the monomeric peroxiredoxin Q class lack these aromatic residues, having hydrophilic or ionizable residues incorporated in their place.[40] Thus, available structural and bioinformatic analyses suggest that these residues are key conserved determinants of oligomerization among particular groups of peroxiredoxins. Moreover, a molecular dynamics study with tryparedoxin peroxidase, a typical 2-Cys peroxiredoxin, pinpointed these conserved aromatic residues (i.e., F48 and Y82) between the subunits as potentially contributing to oligomerization, peroxidatic cysteine reactivity, and protein conformational changes that occur during the catalytic cycle.[41]

Disrupting the decameric structure formed by peroxiredoxins via mutagenesis has enabled the structural analysis of peroxiredoxin-sulfiredoxin complexes, as well as analysis of how particular residues impact peroxidase and chaperone activity.[29,38,42–46] While no mutational studies to our knowledge have been reported on the aromatic residue located at position 44 in Tsa1, two different studies have focused on how the conserved aromatic residue at position 78 in Tsa1 influences the structural states and biochemical activities. In particular, substitution of Tyr78 to Ala in Tsa1 disrupted the decameric structure and yielded a protein with undetectable peroxidase activity in a coupled activity assay.[29] Substitution of the homologous site (i.e., Phe84) in a 2-Cys peroxiredoxin from *Arabidopsis thalania* with Arg resulted in a dimeric protein with comparable peroxidase kinetic properties to that of the wt protein in vitro.[45] In agreement with the results presented herein, the normally decameric form of the protein was shifted to a principally dimeric state when substitutions were introduced at this position. However, on a biochemical level, substitution of this residue with smaller hydrophobic residues (either Ala or Leu) in our studies yielded a partially active protein in vitro, an intermediate effect when considering previous reports. Moreover, our in vivo analysis of Tsa1 harboring mutations that partially disrupt the decameric state correlate closely with the biochemical results for the same proteins, highlighting an intermediate level of cellular and biochemical activity for these proteins, when compared with the wt protein or fully dimeric forms.

Although the Ala substitution of residue 78 in Tsa1 resulted in a protein that retained modest activity, Leu substitutions at either site enhanced biological activity when compared with the corresponding Ala substitution. Others have suggested that Tyr78 participates in decamer formation by forming a unique π-ring/H-bonding relationship with the methylene group in Thr45 to assist in catalysis.[29] Our results indicate that maintaining a hydrophobic interaction

at this site may be as or more important than the previously described hydrogen-bonding interaction, since the $Y^{78}L$ variant of the protein forms a “partially assembled” metastable decamer that possesses a base level of enzymatic activity. The weakened interactions at the decamer–building interface may also account for the temperature-sensitive phenotypic rescue that is observed for this protein, a finding that could be exploited as a conditional tool for understanding the diverse cellular phenotypes associated with *TSA1* deletion or for further development of peroxiredoxin-based redox sensors (e.g., as a potential “on–off” switch).[47,48]

The observation that proteins harboring Leu substitutions at position 44 or Leu or Ala substitutions at position 78 still exhibit activity in vivo is perplexing, given that previous work indicated Tsa1 with the $Y^{78}A$ substitution is inactive in a coupled assay with thioredoxin, thioredoxin reductase, and NADPH.[29] While the rate of reaction with peroxide for each of these proteins is about an order of magnitude lower than that of the wt protein (Figure 5, Table 2), there may also be decreased interaction with, and reduction by, thioredoxins, thereby slowing overall turnover of peroxide by this multienzyme system. Indeed, our cross-linking studies with DVSF indicate that the decamer interface variants of Tsa1 associate less favorably with thioredoxin in cells (see Figure S2 in the Supporting Information, as well as Figure 6). Thus, the combined effects of slow reactivity with H_2O_2 and decreased interaction with Trx may explain the inactivity of this protein in the coupled-activity assay.[29] Alternative disulfide reduction mechanisms, including reduction mediated by the glutaredoxin machinery, exist in the cells.[49] These secondary means of protein disulfide reduction may account for why some decamer interface mutants of Tsa1 partially complement the phenotypes associated with deletion of *TSA1* and *TSA2* in yeast.

Taken together, our results indicate that specific residues at the decamer–building interface contribute to quaternary structure and oxidant defense, but the question as to why typical 2-Cys peroxiredoxins form decamers remains. One potential reason for the correlation between decamer formation and activity is that decamer formation may prime the peroxidatic cysteine for catalysis by maintaining a “fully folded” active site architecture and allowing the pK_a of the catalytic thiol to be depressed via a buttressing effect.[44,46,50] Another explanation for the association of peroxiredoxin activity with an intact decamer is that it may lead to intersubunit cooperativity. Several structures of reduced peroxiredoxins in their decameric state indicate that the individual active sites around the decamer are asymmetrical.[41,51] These differences suggest that the individual subunits may communicate structural information to each other in a cooperative manner; however, positive cooperativity between subunits has not been thoroughly investigated for decameric peroxiredoxins, perhaps because of the complexity of studying such events in a coupled enzyme system. Maintaining the decamer–building interface could also decrease the formation (or increase repair of) of hyperoxidized forms of peroxiredoxin, thereby enabling enhanced activity of wt Tsa1. While another decamer-stabilizing residue can influence AhpC hyperoxidation status when substituted,[46] it is unlikely with the mutants studied here, given the slow initial rate of reactivity with peroxide. However, our experiments do not rule out this possibility.

While the oxidative half-reaction performed by Tsa1 and related proteins is affected by decamer formation, the effect of oligomerization on reductive half-reactions should also be

considered. Since most decameric peroxiredoxins are thought to dissociate to dimers upon oxidation, it is counterintuitive to think that disruption of the decameric state may also impair reduction of the disulfide. Yet, such an observation has been made with variants of the decameric peroxiredoxin AhpC. Specific AhpC variants that form more-stable decamers under oxidizing conditions are more rapidly reduced by the reductase AhpF, whereas certain AhpC variants that prefer a dimeric state upon oxidation are reduced at slower rates.[38] Consistent with these findings, we observed decreased cross-linking between thioredoxin and Tsa1 variants bearing substitutions of aromatic residues at the decamer–building interface, indicating that the reductive half of the catalytic cycle may also be impaired. Collectively, our biological and biochemical work underscores the importance of maintaining the toroid decamer organization for 2-Cys peroxiredoxins, potentially contributing to multiple steps in their catalytic cycles.

Supplementary Material

Refer to Web version on PubMed Central for supplementary material.

ACKNOWLEDGMENTS

We thank Nayun Kim (UT–Houston McGovern Medical School) for helpful suggestions on measuring mutation rates in yeast, Derek Parsonage, Kim Nelson, and Leslie Poole (Wake Forest School of Medicine) for advice on enzymatic assays, and Seth Kelly (The College of Wooster) for advice about quantifying Tsa1 variant expression levels.

Funding

This work was supported by grants from the NIH (Nos. R01-GM127287 (to K.A.M.) and R01-GM072866 (to W.T.L.)) and from the Mindlin Foundation (Undergraduate Mentored Research Award MF15-UMR06 to M.A.L. and J.D.W. and Unsolicited Research Award No. MF16-US03 to J.D.W.). We also acknowledge support from the Henry Luce III Fund for Distinguished Scholarship (to J.D.W.), William H. Wilson Research Funds (to J.D.W.), and the Henry J. Copeland Fund for Independent Study from The College of Wooster. M.A.L., K.M.A., and J.A.B. were supported by the Sophomore Research Program from The College of Wooster. J.E.H. was supported by the Graduate School of Biomedical Sciences at University of Texas Health Science Center at Houston.

ABBREVIATIONS

ROS	reactive oxygen species
Trx	thioredoxin
SEC	size exclusion chromatography
MALS	multiangle light scattering
DVSF	divinyl sulfone
HRP	horseradish peroxidase
wt	wild type

REFERENCES

(1). Finkel T, and Holbrook NJ (2000) Oxidants, oxidative stress and the biology of ageing. Nature 408, 239–247. [PubMed: 11089981]

(2). Brewer TF, Garcia FJ, Onak CS, Carroll KS, and Chang CJ (2015) Chemical approaches to discovery and study of sources and targets of hydrogen peroxide redox signaling through NADPH oxidase proteins. Annu. Rev. Biochem. 84, 765–790. [PubMed: 26034893]

(3). Finkel T (2003) Oxidant signals and oxidative stress. Curr. Opin. Cell Biol. 15, 247–254. [PubMed: 12648682]

(4). Winterbourn CC, and Hampton MB (2008) Thiol chemistry and specificity in redox signaling. Free Radical Biol. Med. 45, 549–561. [PubMed: 18544350]

(5). Veal EA, Day AM, and Morgan BA (2007) Hydrogen peroxide sensing and signaling. Mol. Cell 26, 1–14. [PubMed: 17434122]

(6). D'Autreaux B, and Toledano MB (2007) ROS as signalling molecules: mechanisms that generate specificity in ROS homeostasis. Nat. Rev. Mol. Cell Biol. 8, 813–824. [PubMed: 17848967]

(7). Marnett LJ, Riggins JN, and West JD (2003) Endogenous generation of reactive oxidants and electrophiles and their reactions with DNA and protein. J. Clin. Invest. 111, 583–593. [PubMed: 12618510]

(8). Paulsen CE, and Carroll KS (2013) Cysteine-mediated redox signaling: chemistry, biology, and tools for discovery. Chem. Rev. 113, 4633–4679. [PubMed: 23514336]

(9). Garcia-Santamarina S, Boronat S, and Hidalgo E (2014) Reversible cysteine oxidation in hydrogen peroxide sensing and signal transduction. Biochemistry 53, 2560–2580. [PubMed: 24738931]

(10). Cremers CM, and Jakob U (2013) Oxidant sensing by reversible disulfide bond formation. J. Biol. Chem. 288, 26489–26496. [PubMed: 23861395]

(11). Winterbourn CC (2013) The biological chemistry of hydrogen peroxide. Methods Enzymol. 528, 3–25. [PubMed: 23849856]

(12). Poole LB (2015) The basics of thiols and cysteines in redox biology and chemistry. Free Radical Biol. Med. 80, 148–157. [PubMed: 25433365]

(13). Hall A, Karplus PA, and Poole LB (2009) Typical 2-Cys peroxiredoxins: structures, mechanisms and functions. FEBS J. 276, 2469–2477. [PubMed: 19476488]

(14). Rhee SG, Woo HA, Kil IS, and Bae SH (2012) Peroxiredoxin functions as a peroxidase and a regulator and sensor of local peroxides. J. Biol. Chem. 287, 4403–4410. [PubMed: 22147704]

(15). Lu J, and Holmgren A (2014) The thioredoxin antioxidant system. Free Radical Biol. Med. 66, 75–87. [PubMed: 23899494]

(16). Wood ZA, Schroder E, Robin Harris J, and Poole LB (2003) Structure, mechanism and regulation of peroxiredoxins. Trends Biochem. Sci. 28, 32–40. [PubMed: 12517450]

(17). Kumsta C, and Jakob U (2009) Redox-regulated chaperones. Biochemistry 48, 4666–4676. [PubMed: 19368357]

(18). Rhee SG, and Kil IS (2017) Multiple functions and regulation of mammalian peroxiredoxins. Annu. Rev. Biochem. 86, 749–775. [PubMed: 28226215]

(19). Stocker S, Van Laer K, Mijuskovic A, and Dick TP (2018) The conundrum of hydrogen peroxide signaling and the emerging role of peroxiredoxins as redox relay hubs. Antioxid. Redox Signaling 28, 558–573.

(20). Hall A, Nelson K, Poole LB, and Karplus PA (2011) Structure-based insights into the catalytic power and conformational dexterity of peroxiredoxins. Antioxid. Redox Signaling 15, 795–815.

(21). Chae HZ, Kim IH, Kim K, and Rhee SG (1993) Cloning, sequencing, and mutation of thiol-specific antioxidant gene of Saccharomyces cerevisiae. J. Biol. Chem. 268, 16815–16821. [PubMed: 8344960]

(22). Lee J, Spector D, Godon C, Labarre J, and Toledano MB (1999) A new antioxidant with alkyl hydroperoxide defense properties in yeast. J. Biol. Chem. 274, 4537–4544. [PubMed: 9988687]

(23). Wong CM, Siu KL, and Jin DY (2004) Peroxiredoxin-null yeast cells are hypersensitive to oxidative stress and are genomically unstable. J. Biol. Chem. 279, 23207–23213. [PubMed: 15051715]

(24). Tachibana T, Okazaki S, Murayama A, Naganuma A, Nomoto A, and Kuge S (2009) A major peroxiredoxin-induced activation of Yap1 transcription factor is mediated by reduction-sensitive disulfide bonds and reveals a low level of transcriptional activation. J. Biol. Chem. 284, 4464–4472. [PubMed: 19106090]

(25). Munhoz DC, and Netto LE (2004) Cytosolic thioredoxin peroxidase I and II are important defenses of yeast against organic hydroperoxide insult: catalases and peroxiredoxins cooperate in the decomposition of H_2O_2 by yeast. J. Biol. Chem. 279, 35219–35227. [PubMed: 15210711]

(26). Lian FM, Yu J, Ma XX, Yu XJ, Chen Y, and Zhou CZ (2012) Structural snapshots of yeast alkyl hydroperoxide reductase Ahp1 peroxiredoxin reveal a novel two-cysteine mechanism of electron transfer to eliminate reactive oxygen species. J. Biol. Chem. 287, 17077–17087. [PubMed: 22474296]

(27). Tairum CA Jr., de Oliveira MA, Horta BB, Zara FJ, and Netto LES (2012) Disulfide biochemistry in 2-Cys peroxiredoxin: requirement of Glu50 and Arg146 for the reduction of yeast Tsa1 by thioredoxin. J. Mol. Biol. 424, 28–41. [PubMed: 22985967]

(28). Jang HH, Lee KO, Chi YH, Jung BG, Park SK, Park JH, Lee JR, Lee SS, Moon JC, Yun JW, Choi YO, Kim WY, Kang JS, Cheong GW, Yun DJ, Rhee SG, Cho MJ, and Lee SY (2004) Two enzymes in one: two yeast peroxiredoxins display oxidative stress-dependent switching from a peroxidase to a molecular chaperone function. Cell 117, 625–635. [PubMed: 15163410]

(29). Tairum CA, Santos MC, Breyer CA, Geyer RR, Nieves CJ, Portillo-Ledesma S, Ferrer-Sueta G, Toledo JC Jr., Toyama MH, Augusto O, Netto LE, and de Oliveira MA (2016) Catalytic Thr or Ser residue modulates structural switches in 2-Cys peroxiredoxin by distinct mechanisms. Sci. Rep. 6, 33133. [PubMed: 27629822]

(30). Perkins A, Nelson KJ, Parsonage D, Poole LB, and Karplus PA (2015) Peroxiredoxins: guardians against oxidative stress and modulators of peroxide signaling. Trends Biochem. Sci. 40, 435–445. [PubMed: 26067716]

(31). Allan KM, Loberg MA, Chepngeno J, Hurtig JE, Tripathi S, Kang MG, Allotey JK, Widdershins AH, Pilat JM, Sizek HJ, Murphy WJ, Naticchia MR, David JB, Morano KA, and West JD (2016) Trapping redox partnerships in oxidant-sensitive proteins with a small, thiol-reactive cross-linker. Free Radical Biol. Med. 101, 356–366. [PubMed: 27816612]

(32). Naticchia MR, Brown HA, Garcia FJ, Lamade AM, Justice SL, Herrin RP, Morano KA, and West JD (2013) Bifunctional electrophiles cross-link thioredoxins with redox relay partners in cells. Chem. Res. Toxicol. 26, 490–497. [PubMed: 23414292]

(33). West JD, Stamm CE, Brown HA, Justice SL, and Morano KA (2011) Enhanced toxicity of the protein cross-linkers divinyl sulfone and diethyl acetylenedicarboxylate in comparison to related monofunctional electrophiles. Chem. Res. Toxicol. 24, 1457–1459. [PubMed: 21812477]

(34). Schindelin J, Arganda-Carreras I, Frise E, Kaynig V, Longair M, Pietzsch T, Preibisch S, Rueden C, Saalfeld S, Schmid B, Tinevez JY, White DJ, Hartenstein V, Eliceiri K, Tomancak P, and Cardona A (2012) Fiji: an open-source platform for biological-image analysis. Nat. Methods 9, 676–682. [PubMed: 22743772]

(35). Huang ME, Rio AG, Nicolas A, and Kolodner RD (2003) A genomewide screen in *Saccharomyces cerevisiae* for genes that suppress the accumulation of mutations. Proc. Natl. Acad. Sci. U. S. A 100, 11529–11534. [PubMed: 12972632]

(36). Ogusucu R, Rettori D, Munhoz DC, Soares Netto LE, and Augusto O (2007) Reactions of yeast thioredoxin peroxidases I and II with hydrogen peroxide and peroxynitrite: rate constants by competitive kinetics. Free Radical Biol. Med. 42, 326–334. [PubMed: 17210445]

(37). West JD, Roston TJ, David JB, Allan KM, and Loberg MA (2018) Piecing together how peroxiredoxins maintain genomic stability. Antioxidants 7, 177.

(38). Nelson KJ, Perkins A, Van Swearingen AED, Hartman S, Brereton AE, Parsonage D, Salsbury FR Jr., Karplus PA, and Poole LB (2018) Experimentally dissecting the origins of peroxiredoxin catalysis. Antioxid. Redox Signaling 28, 521–536.

(39). Karplus PA, and Hall A (2007) Structural survey of the peroxiredoxins. Subcell. Biochem. 44, 41–60. [PubMed: 18084889]

(40). Reeves SA, Parsonage D, Nelson KJ, and Poole LB (2011) Kinetic and thermodynamic features reveal that *Escherichia coli* BCP is an unusually versatile peroxiredoxin. Biochemistry 50, 8970–8981. [PubMed: 21910476]

(41). Yuan Y, Knaggs M, Poole L, Fetrow J, and Salsbury F Jr. (2010) Conformational and oligomeric effects on the cysteine pK_a of tryparedoxin peroxidase. J. Biomol. Struct. Dyn. 28, 51–70. [PubMed: 20476795]

(42). Jonsson TJ, Johnson LC, and Lowther WT (2008) Structure of the sulphiredoxin-peroxiredoxin complex reveals an essential repair embrace. Nature 451, 98–101. [PubMed: 18172504]

(43). Jonsson TJ, Johnson LC, and Lowther WT (2009) Protein engineering of the quaternary sulfiredoxin-peroxiredoxin enzyme-substrate complex reveals the molecular basis for cysteine sulfinic acid phosphorylation. J. Biol. Chem. 284, 33305–33310. [PubMed: 19812042]

(44). Parsonage D, Youngblood DS, Sarma GN, Wood ZA, Karplus PA, and Poole LB (2005) Analysis of the link between enzymatic activity and oligomeric state in AhpC, a bacterial peroxiredoxin. Biochemistry 44, 10583–10592. [PubMed: 16060667]

(45). Konig J, Galliardt H, Jutte P, Schaper S, Dittmann L, and Dietz KJ (2013) The conformational bases for the two functionalities of 2-cysteine peroxiredoxins as peroxidase and chaperone. J. Exp. Bot. 64, 3483–3497. [PubMed: 23828546]

(46). Kamariah N, Eisenhaber B, Eisenhaber F, and Gruber G (2018) Active site CP-loop dynamics modulate substrate binding, catalysis, oligomerization, stability, over-oxidation and recycling of 2-Cys peroxiredoxins. Free Radical Biol. Med. 118, 59–70. [PubMed: 29474868]

(47). Morgan B, Van Laer K, Owusu TN, Ezerina D, Pastor-Flores D, Amponsah PS, Tursch A, and Dick TP (2016) Realtime monitoring of basal H_2O_2 levels with peroxiredoxin-based probes. Nat. Chem. Biol. 12, 437–443. [PubMed: 27089028]

(48). Langford TF, Huang BK, Lim JB, Moon SJ, and Sikes HD (2018) Monitoring the action of redox-directed cancer therapeutics using a human peroxiredoxin-2-based probe. Nat. Commun. 9, 3145. [PubMed: 30087344]

(49). Draculic T, Dawes IW, and Grant CM (2000) A single glutaredoxin or thioredoxin gene is essential for viability in the yeast *Saccharomyces cerevisiae*. Mol. Microbiol. 36, 1167–1174. [PubMed: 10844700]

(50). Wood ZA, Poole LB, Hantgan RR, and Karplus PA (2002) Dimers to doughnuts: redox-sensitive oligomerization of 2-cysteine peroxiredoxins. Biochemistry 41, 5493–5504. [PubMed: 11969410]

(51). Salsbury FR Jr., Yuan Y, Knaggs MH, Poole LB, and Fetrow JS (2012) Structural and electrostatic asymmetry at the active site in typical and atypical peroxiredoxin dimers. J. Phys. Chem. B 116, 6832–6843. [PubMed: 22401569]

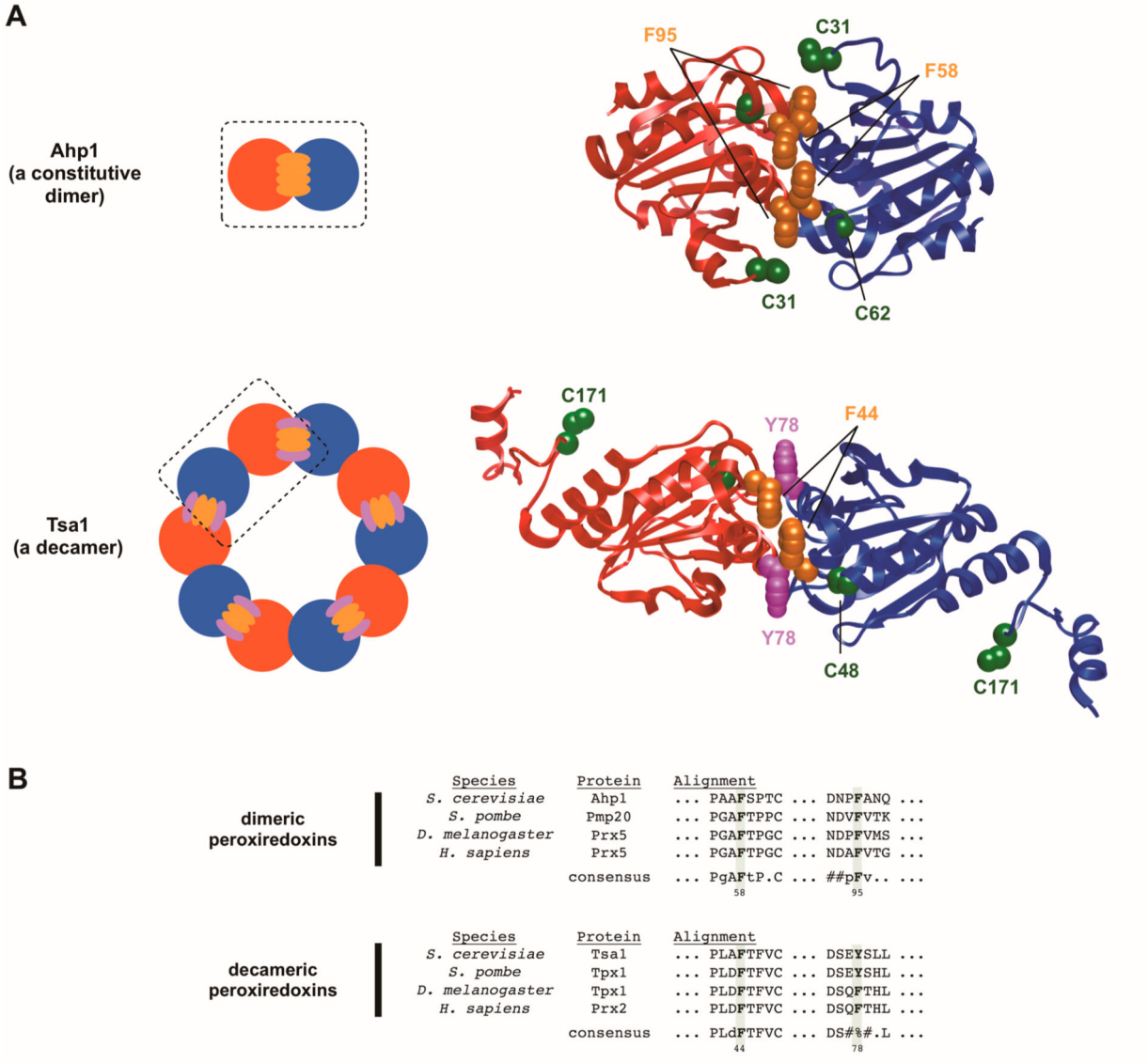

Figure 1.

Comparison of oligomerization interfaces between Ahp1 and Tsa1. (A) Structural comparison depicting where the A-type interface residues in Ahp1 and Tsa1 that are examined in this study are located. In each simplified diagram, the functional dimer wherein intersubunit disulfide bonds are formed is shown as a dashed box. Phenylalanine or tyrosine residues investigated in this study are highlighted in orange or pink, respectively. Catalytic cysteine residues involved in intersubunit disulfide formation are depicted in green. Structural depictions were generated using Chimera software (https://www.cgl.ucsf.edu/chimera/) from the Protein Databank files 4DSR (Ahp1) and 3SBC (Tsa1).[26,27] (B) Sequence alignments of conserved aromatic residues at the A-type dimer interface in Ahp1 and the A-type decamer–building interface in Tsa1.

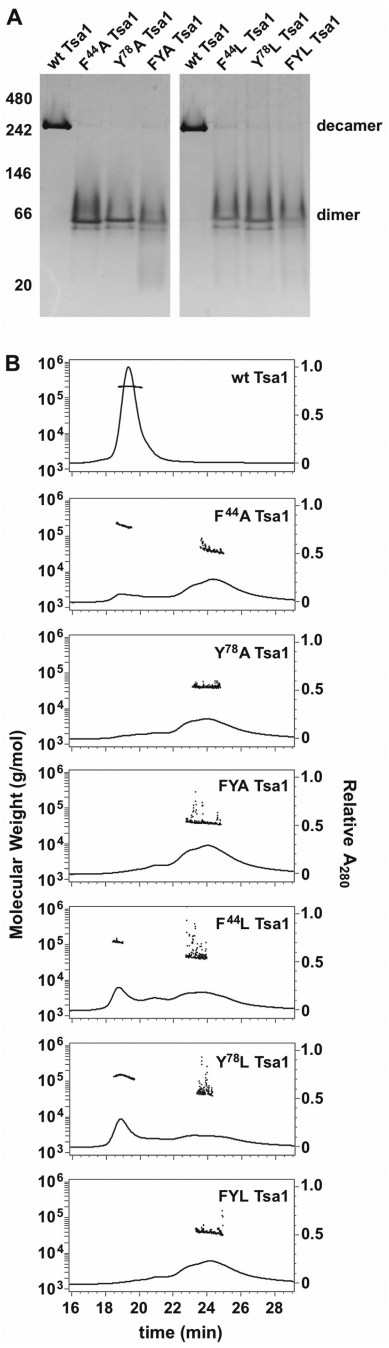

Figure 2.

Mutation of conserved aromatic residues at the Tsa1 decamer interface disrupts its quaternary structure. (A) Purified proteins were diluted to 10 μM, resolved on native PAGE, and visualized by staining with Coomassie Blue. (B) Purified proteins were diluted to 100 μM in buffer containing 20 mM HEPES (pH 7.5), 100 mM NaCl, and 1 mM TCEP prior to resolution and analysis by SEC-MALS. Traces depict A_{280} values (right y-axis) over the duration of the separation, whereas approximate molecular weights of specific peaks

(corresponding to values on the left y-axis) are indicated as scatter plots within or above individual peaks. Results are representative of three independent experiments.

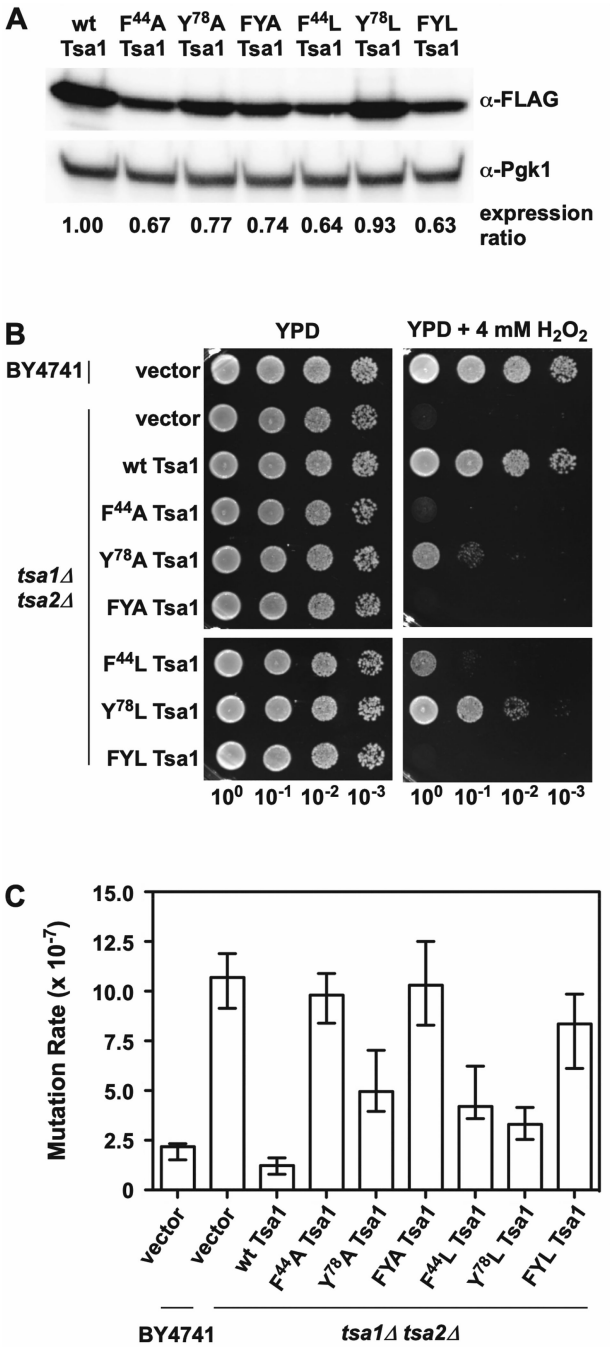

Figure 3.

Substitution of conserved aromatic residues at the Tsa1 decamer interface compromise the protein's ability to protect against oxidants and genomic instability. (A) Expression levels of decamer interface variants were compared with that of wt Tsa1 via immunoblot. Pgk1 levels were monitored as a loading control. (B) Decamer interface variants of Tsa1 were tested for their ability to prevent peroxide-mediated toxicity. Strains were grown to stationary phase, diluted serially before plating on YPD medium or YPD medium containing 4 mM H_2O_2, and grown for 48 h at 30 °C. Results are representative of three independent experiments.

(C) Strains expressing Tsa1 decamer interface variants were monitored for spontaneous mutation of the gene encoding the arginine transporter (*CAN1*) as described in the Materials and Methods section. Results shown are the median mutation rate ±95% confidence limit for two independent trials, each performed with nine individual isolates of the indicated strain.

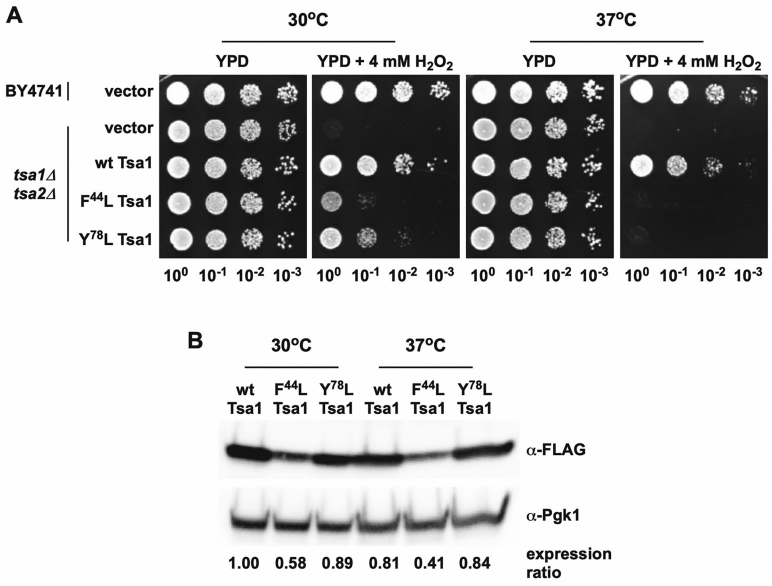

Figure 4.

Phenotypic rescue by Tsa1 variants forming partial decamers is temperature-sensitive. (A) Yeast strains expressing partially functional Tsa1 variants were assayed for temperature sensitivity by plating serial dilutions on YPD or YPD + 4 mM H_2O_2 and incubating at 30 or 37 °C for 48 h. (B) Temperature-sensitive variants of Tsa1 were expressed in *tsa1*Δ*tsa2*Δ cells were monitored for stability at 30 or 37 °C, following growth of cultures for 8 h at the indicated temperature. FLAG-tagged Tsa1 proteins were detected by immunoblot. Pgk1 levels were monitored as a loading control. Results are representative of three independent experiments.

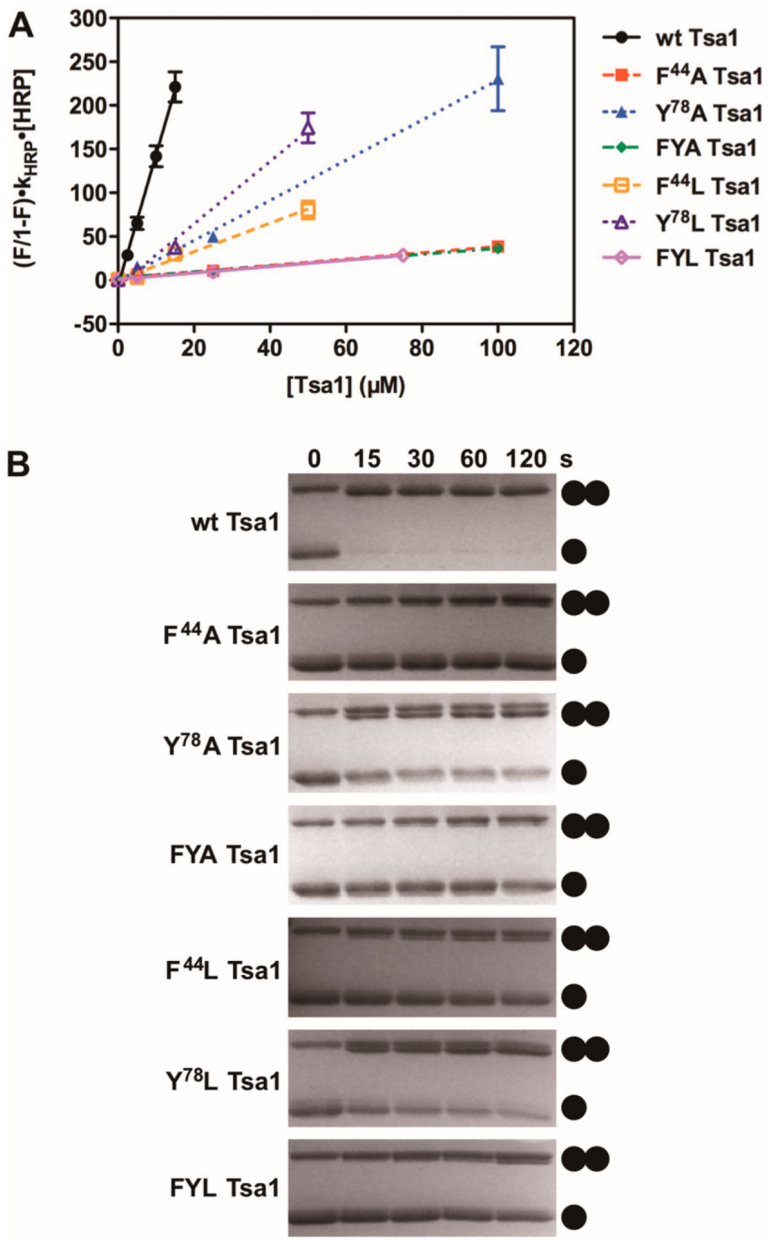

Figure 5.

Decamer interface variants of Tsa1 react more slowly with H_2O_2. (A) Samples containing 3.75 μM horseradish peroxidase (HRP) and varying concentrations of Tsa1 were incubated with 3 μM H_2O_2 and immediately measured at 403 nm for loss of HRP absorbance. The relative decrease in A_{403} was determined for each sample. Second-order rate constants for reactivity of each Tsa1 variant with H_2O_2 were calculated from the slope of the line (reported in Table 2). Data points represent the average of three independent experiments, each conducted in quadruplicate, ± the standard error of mean (±SEM). The curves for $F^{44}A$ Tsa1, FYA Tsa1, and FYL Tsa1 have the smallest slopes and overlap considerably, reflected in their similar k_{SOH} values. (B) Tsa1 variants were reduced with DTT, desalted, and diluted to 10 μM prior to incubation for the indicated times with 15 μM H_2O_2 at room temperature.

Proteins were denatured in nonreducing sample buffer and resolved by SDS-PAGE. Results are representative of three independent experiments.

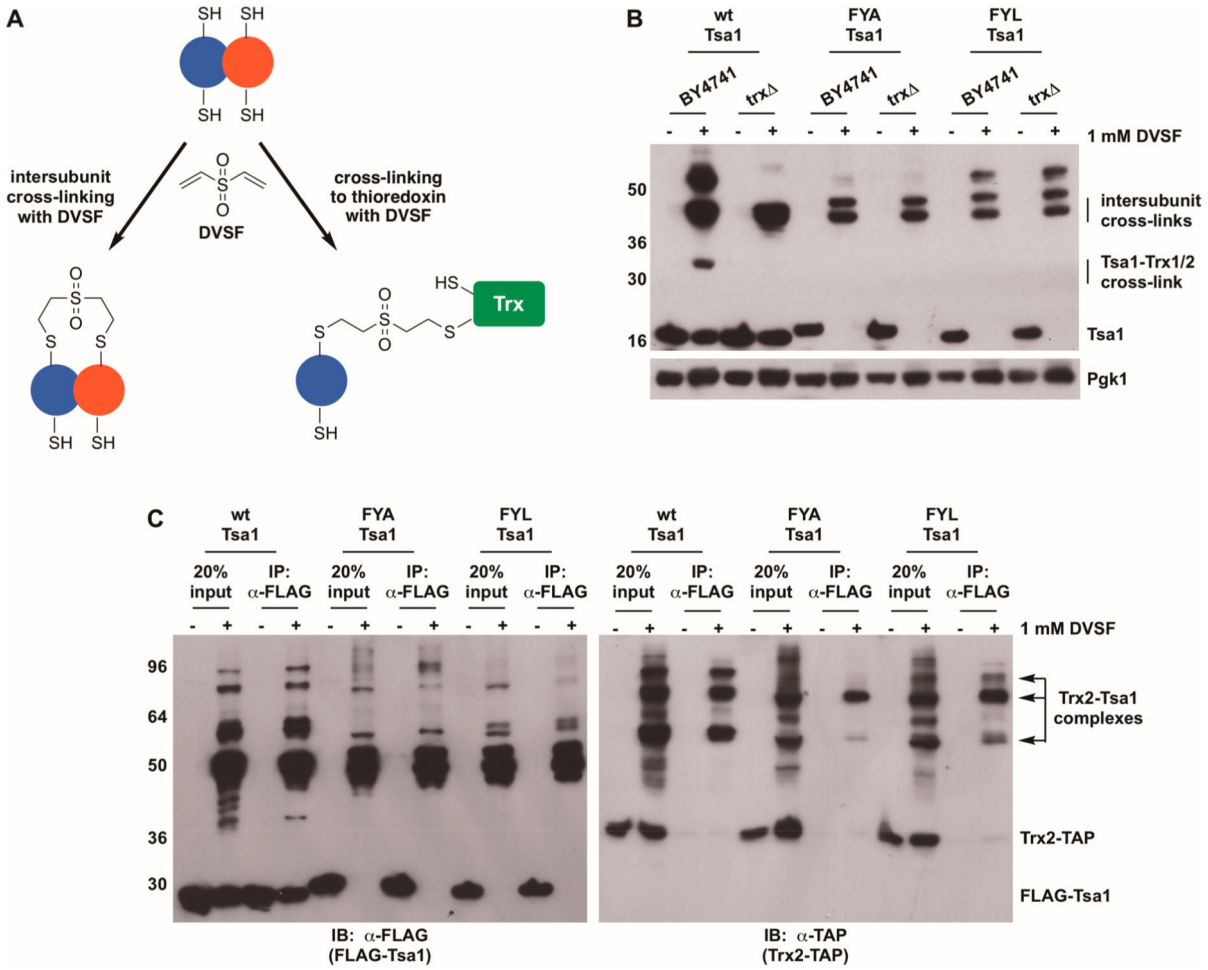

Figure 6.

Tsa1 decamer interface variants undergo less DVSF-mediated cross-linking to thioredoxin. (A) Possible cross-linking reactions that Tsa1 undergoes in cells treated with the bifunctional electrophile DVSF. (B) Wild-type cells (BY4741) or cells lacking Trx1 and Trx2 (*trx*Δ) expressing FLAG-tagged Tsa1 variants were treated with 1 mM DVSF for 1 h at 30 °C. FLAG-tagged Tsa1 and its cross-linked species were detected via immunoblot. Pgk1 levels were monitored as a loading control. (C) FLAG-tagged Tsa1 variants were expressed in cells containing a TAP-tagged Trx2 and were subsequently immunoprecipitated from cell lysates treated with DVSF. Immunoprecipitates were probed with antibodies against the FLAG or TAP tags via immunoblot. Results are representative of three independent experiments.

Table 1.

Estimated Molecular Weights of Tsa1 Species from SEC-MALS Analysis[a]

protein	retention time (~19 min), Peak 1 (g/mol)	retention time (~24 min), Peak 2 (g/mol)
wt Tsa1	212 900	–
$F^{44}A$ Tsa1	210 300	40 250
$Y^{78}A$ Tsa1	–	41 790
FYA Tsa1	–	36 920
$F^{44}L$ Tsa1	116 800	51 480
$Y^{78}L$ Tsa1	150 600	46 340
FYL Tsa1	–	39 770

[a]Molecular weights were estimated by MALS analysis of protein complexes upon elution from the size exclusion column. The predicted molecular weight of the Tsa1 decamer is 227 kDa, whereas the predicted molecular weight of a dimer is 45.4 kDa.

Table 2.

Second-Order Rate Constants for Tsa1 Variants Reacting with H_2O_2[a]

protein	k_{SOH} (M^{-1} s^{-1})
wt Tsa1	$1.5 \pm 0.1 \times 10^7$
$F^{44}A$ Tsa1	$3.6 \pm 0.4 \times 10^5$
$Y^{78}A$ Tsa1	$2.3 \pm 0.2 \times 10^6$
FYA Tsa1	$3.4 \pm 0.4 \times 10^5$
$F^{44}L$ Tsa1	$1.6 \pm 0.2 \times 10^6$
$Y^{78}L$ Tsa1	$3.6 \pm 0.2 \times 10^6$
FYL Tsa1	$3.7 \pm 0.4 \times 10^5$

[a]Rate constants were determined from a competition assay with HRP, as described in the Materials and Methods section. Values shown are the slope of the lines from Figure 4A.